ELSEVIER

International Journal of Heat and Fluid Flow 19 (1998) 326–337

International Journal of HEAT AND FLUID FLOW

A strain parameter turbulence model and its application to homogeneous and thin shear flows

M.A. Cotton *, J.O. Ismael

School of Engineering, University of Manchester, Oxford Road, Manchester M13 9PL, UK

Received 27 September 1997; accepted 12 February 1998

Abstract

The present paper examines the basic tenets upon which widely-used two-equation (k–ϵ) turbulence models are based. It is argued that there exists a weakness at the core of this group of models, namely in the assumed stress/rate-of-strain constitutive equation. These remarks apply to both the 'high-Reynolds-number' parent model and to 'low-Reynolds-number' variants of the formulation. Dimensional considerations and the work of Lee et al. (Proceedings of the Sixth Symposium on Turbulent Shear Flows, 1987; J. Fluid Mech. 216 (1990) 561–583) support the contention that the constitutive relation should take account of the ratio of turbulence to mean strain timescales. In an extension of this approach, following Townsend (J. Fluid Mech. 41 (1970) 13–46) and Maxey (J. Fluid Mech. 124 (1982) 261–282), the concept of effective total strain is introduced. A 'strain parameter', S, is then defined as the subject of a third transport equation and a new turbulence model damping function is made to depend principally upon S. The model is compared with data for homogeneous flow transients, steady fully-developed channel flow, and mixed convection flows.

Keywords: Channel flow; Flow timescales; Homogeneous flow; Mixed convection; Rapid distortion; Strain parameter; Total strain

Notation

a,b,c	constants
c_p	specific heat capacity at constant pressure
$C_{\epsilon 1}$, $C_{\epsilon 2}$	constants in ϵ-equation
C_μ	constant in constitutive equation
D	pipe diameter
F_1, F_2	functions
g	acceleration due to gravity
Gr	Grashof number, $\beta g \dot{q} D^4/\lambda \nu^2$
H	channel half-width
Nu	Nusselt number, $\dot{q}D/\lambda(\theta_w - \theta_b)$
p	pressure
Pr	Prandtl number, $c_p\mu/\lambda$
$\dot{q}$	wall heat flux
Re	Reynolds number, $2U_bH/\nu$ or U_bD/ν.
Re_t	turbulent Reynolds number
t	time
U,V	mean velocities in x-, y-directions
u,v	fluctuating velocities in x-, y-directions
U_i, u_i	mean, fluctuating velocity components in Cartesian tensors
U_τ	friction velocity, $(\tau_w/\rho)^{1/2}$
x	streamwise coordinate
y	cross-stream (wall normal) coordinate
y^+	yU_τ/ν

Greek

β	coefficient of volumetric expansion
δ_{ij}	Kronecker delta
$\tilde{\epsilon}$	modified dissipation variable, $\tilde{\epsilon} = \epsilon - D_\epsilon$
θ	absolute temperature
λ	thermal conductivity
μ	dynamic viscosity
ν	kinematic viscosity, μ/ρ
ρ	density
σ_k, σ_ϵ	turbulent Prandtl number for diffusion of k,ϵ
τ	shear stress

Subscripts

b	bulk
t	turbulent
w	wall

Superscript

$\bar{}$	time-average (steady flows) or ensemble-average (unsteady flows)

Other symbols are defined in the text.

1. Introduction

The desire to have available relatively simple means of computing practically-important turbulent flows has provided an

* Corresponding author.

PII: S0142-727X(98)10003-6

impetus for the sustained development and application of turbulence models. Current practice to devise averaged turbulence models of a closed mathematical form is based almost entirely on two strategies, both of which were first formulated in detail some 20 years ago: (i) k–ϵ turbulent viscosity models in which transport equations are solved for the turbulent kinetic energy, k and its rate of dissipation, ϵ, and (ii) Reynolds stress transport models in which modelled equations for the individual stress components are solved in conjunction with the ϵ-equation. The former, less complex, group of models have found particularly widespread application and the present study examines the fundamentals of k–ϵ modelling and advances a formulation of a k–ϵ–strain parameter model.

A group which is key to the present work is the dimensionless strain rate, $(k/\epsilon)\partial U/\partial y$ (which, as discussed below, may also be considered either as a timescale ratio or as a total strain): in particular it appears that the variation of the group across the buffer layer ($5 < y^+ < 60$) of wall-bounded flows may be closely associated with the correct distribution of a 'damping function' (or modifier of the k–ϵ model C_μ constant). The strongest evidence in support of the role of the dimensionless strain rate is supplied by the Direct Numerical Simulation (DNS) studies of Lee et al. (1987, 1990) who related the group to the characterization of both instantaneous flow realizations and structural statistics (ratios such as $-\overline{uv}/k$) of turbulence. Lee et al. demonstrated that similar flow features arise in homogeneous shear flows and regions of steady wall-bounded flows under conditions where values of the dimensionless strain rate are approximately matched. The results of dimensional analysis lend further support to the argument that $(k/\epsilon)\partial U/\partial y$ is a critical local parameter in relation to wall-bounded flows. Now, $(k/\epsilon)\partial U/\partial y$ is the total strain arising from the application of the mean flow strain rate, $\partial U/\partial y$ over the timescale of large-scale turbulence, k/ϵ. At times short in relation to the large-scale timescale, the results of Rapid Distortion Theory (RDT) indicate that structural statistics of turbulence depend upon the actual total strain, $t\cdot\partial U/\partial y$. (RDT is based upon a linearization of the Navier–Stokes equations and is formally valid where strain rates are high or elapsed distortion times short; reviews of RDT are provided by Hunt, 1978, Savill, 1987, Hunt and Carruthers, 1990.) Maxey (1982), following the earlier work of Townsend (1970), advanced an ad hoc equation for effective total strain, α_{eff}. The physical significance of the α_{eff}-equation lies in the values it returns at the asymptotic limits of short and long distortion times: in terms of the present modelling parameters, α_{eff} approximates to $t\cdot\partial U/\partial y$ at short times ($t/(k/\epsilon) \ll 1$); at longer times α_{eff} is truncated on $(k/\epsilon)\partial U/\partial y$. Maxey coupled the effective total strain equation with a relation for $-\overline{uv}/k$ in terms of α_{eff}. Thus, over short elapsed times, the structural ratio depends only on total strain; at longer times the ratio is a function of $(k/\epsilon)\partial U/\partial y$. It follows that the approach is in accordance with RDT and also encompasses the dependence identified by Lee et al. under longer-time conditions.

The concept of effective total strain is developed below to obtain an equation for a strain parameter, here denoted S. The strain parameter is made the independent variable of a damping function $f_S(S)$ such that the Reynolds stress may be determined within the framework of a conventional engineering turbulence model: $-\overline{uv} = C_\mu f_S(S)(k^2/\epsilon)\partial U/\partial y$. Clearly, under conditions where $f_S(S) = 1$ the constitutive equation of the standard k–ϵ model is recovered.

2. Model development

The present section commences with a brief review of established practice in the computation of turbulent flows using two-equation turbulent viscosity closures (Section 2.1). The timescales of large-scale turbulence and of mean flow straining are considered in Section 2.2 and reference is made to the observations of Lee et al. (1987, 1990). The effective total strain equations of Townsend (1970) and Maxey (1982) are then considered and the present strain parameter equation is developed. Finally, Section 2.3 details the 3-equation strain parameter turbulence model for application to flows with a single (or principal) strain rate, $\partial U/\partial y$.

2.1. Current practice in turbulent viscosity modelling

Turbulent viscosity models relate the Reynolds stress $-\overline{uv}$ to the mean strain field by employing a constitutive equation:

$$-\overline{uv} = \nu_t \frac{\partial U}{\partial y}. \tag{1}$$

A number of researchers (see for example Speziale, 1987 and Craft et al., 1996) have made proposals to extend Eq. (1) to include non-linear constructions of the strain rate and vorticity tensors. Non-linear constitutive equations are designed to increase the range of reliable application of turbulent viscosity models, but recover Eq. (1) for the determination of the $-\overline{uv}$ stress component in parallel flows. Current attention is directed towards the specification of ν_t in Eq. (1), but the possibility of subsequent extension to more general flows is noted.

The models employing Eq. (1) fall principally into categories of prescribed eddy diffusivity, mixing length, and one- and two-equation transport models (see Launder and Spalding, 1972). Of those, however, it is only members of the latter group that are widely perceived to afford a realistic possibility of resolving some 'non-universal' flow features (such as departures from the 'law of the wall'). The turbulent kinetic energy and its rate of dissipation are most commonly selected as the subjects of the two scale-determining transport equations. The standard 'high-Reynolds-number' k–ϵ model is presented by Launder and Spalding (1974): turbulent viscosity appearing in Eq. (1) is expressed as

$$\nu_t = C_\mu \frac{k^2}{\epsilon}. \tag{2}$$

Substitution of Eq. (2) in Eq. (1) shows that a linear relationship between $-\overline{uv}/k$ and $(k/\epsilon)\partial U/\partial y$ is effectively postulated in k–ϵ models:

$$-\frac{\overline{uv}}{k} = C_\mu \frac{k}{\epsilon}\frac{\partial U}{\partial y}. \tag{3}$$

In fact, the straight line of Eq. (3) passes through a single experimentally justified point, $[(k/\epsilon)\partial U/\partial y,\ -\overline{uv}/k] = [(0.3)^{-1},\ 0.3]$. These values characterize the logarithmic region of thin shear flows where k production and dissipation rates are approximately balanced and, given the linear relationship above, determine the value of C_μ ($C_\mu = 0.09$).

Eqs. (1) and (2) do not correctly reproduce the observed diminution of Reynolds stress as a wall is approached and in 'low-Reynolds-number' k–ϵ models a multiplier f, termed a damping function, is introduced to the right of Eq. (2). Jones and Launder (1972) proposed the first such model and specified $f = f_\mu$ (Re_t); a revised version of the model due to Launder and Sharma (1974), generally denoted 'LS' below, has been widely applied and is frequently employed as a benchmark against which other two-equation formulations are compared (the LS model is used here for purposes of comparison in Section 3). The level of activity in the development of alternative closures is demonstrated by the papers of Patel et al. (1985), Betts and Dafa'Alla (1986), Savill (1993), Cotton and Kirwin (1993), and Jackson and He (1995) who, amongst others,

review and assess a range of two-equation models. The consensus to be derived from these comparative studies is that the LS model is the most accurate of those tested, although even that model does not exhibit a high degree of quantitative accuracy in a number of applications. Many of the models examined in the studies above use non-local parameters, such as y^+ or $yk^{1/2}/\nu$, as the argument of the damping function. Use of a non-dimensionalized wall distance parameter carries with it an implicit assumption of 'universality' (Reynolds number independence when quantities are considered in '+' variables) and is therefore an intrinsically limited modelling strategy. However, despite the fundamental advantages offered by local Re_t-based models, undue reliance is placed upon the turbulent Reynolds number in order to achieve the required level of damping in regions where viscosity would *not* be expected to a parameter. This apparent failure to reflect the real mechanisms governing near-wall turbulence has been suspected for some time (Launder's, 1986), nonetheless alternative approaches have been slow to appear.

2.2. Flow timescales and effective total strain

Taken in overview, modelling at the k–ϵ level seeks to express the unknown Reynolds stress in terms of the scalar variables and the mean strain field:

$$-\overline{uv} = F_1(k, \epsilon, \partial U/\partial y). \tag{4}$$

Viscous effects are here taken to be negligible, and attention is again restricted to the determination of the $-\overline{uv}$ stress component in the presence of a single steep velocity gradient. Dimensional analysis applied to Eq. (4) indicates that two independent dimensionless groups exist:

$$-\frac{\overline{uv}}{k} = F_2\left(\frac{k}{\epsilon}\frac{\partial U}{\partial y}\right). \tag{5}$$

It is seen that the generally-adopted constitutive equation, Eq. (3), is a special case of Eq. (5). In the more familiar notation of turbulence modelling, the Reynolds stress appearing in Eq. (5) may be expressed as

$$-\overline{uv} = C_\mu f\left(\frac{k}{\epsilon}\frac{\partial U}{\partial y}\right)\frac{k^2}{\epsilon}\frac{\partial U}{\partial y}. \tag{6}$$

k/ϵ represents the timescale of large-scale turbulence and $(\partial U/\partial y)^{-1}$ is the timescale of straining by the mean field. f appearing in Eq. (6) assumes the role of a damping function which is dependent upon the timescale ratio. Lee et al. (1987, 1990) obtained the profile of $(k/\epsilon)\partial U/\partial y$ against y^+ from the DNS channel flow data of Kim et al. (1987). It was found that the group rose from zero at the wall to a pronounced maximum of approximately 17.5 at $y^+ \simeq 10$; beyond that location $(k/\epsilon)\partial U/\partial y$ decreased to approximately 3 (or $C_\mu^{-1/2}$, cf. Section 2.1) at the edge of the buffer layer and maintained that value across the logarithmic region. Thus, in relation to Eq. (6), it is seen that there exists a striking coincidence between the location of the near-wall excursion of the $(k/\epsilon)\partial U/\partial y$ profile and the region where the damping function is operative. In an early exploratory study the present authors (Cotton and Ismael, 1993) developed a k–ϵ model incorporating a damping function of the form indicated by Eq. (6): although some initially encouraging results were obtained, it was necessary to multiply the function $f[(k/\epsilon)\partial U/\partial y]$ by a viscous damping function $f_\mu(Re_t)$ of approximately the same magnitude.

Now, as indicated earlier, the timescale ratio $(k/\epsilon)\partial U/\partial y$ may be viewed alternatively as the total strain corresponding to distortion over the large-scale turbulence timescale. RDT is concerned with distortions over shorter times which led Maxey (1982) to refine a proposal of Townsend (1970) for an equation describing total effective strain, α_{eff}. Hence, for homogeneous flow:

$$\frac{\partial_{\alpha_{\text{eff}}}}{\partial t} = \frac{\partial U}{\partial y} - \frac{\alpha_{\text{eff}}}{T_D}, \tag{7}$$

where T_D is a timescale associated with large-scale turbulence. It is instructive to examine the behaviour of Eq. (7) for the simple case where both T_D and $\partial U/\partial y$ are assumed to be constant: taking the initial condition $\alpha_{\text{eff}} = 0$ at $t = 0$, the solution of the equation is seen to be

$$\alpha_{\text{eff}} = T_D\frac{\partial U}{\partial y}\left[1 - \exp(-t/T_D)\right]. \tag{8}$$

At times short by comparison with the turbulence distortion timescale, $t \ll T_D$, a Taylor series expansion shows α_{eff} to be equal to the total strain $t\cdot\partial U/\partial y$; at longer times, $t \gg T_D$, α_{eff} asymptotes to $T_D\cdot\partial U/\partial y$. Further insight into the properties of Eq. (7) may be gained if the constraint of temporally constant $\partial U/\partial y$ is removed. Thus, with $\partial U/\partial y$ a function of time, the solution of Eq. (7) is obtained as a convolution integral:

$$\alpha_{\text{eff}} = \int_0^t \exp\left(\frac{\tau - t}{T_D}\right)\frac{\partial U}{\partial y}(\tau)\,\mathrm{d}\tau. \tag{9}$$

Eq. (9) succinctly illustrates the quality of receding, or weighted, 'memory' possessed by the Townsend/Maxey α_{eff} variable. At the present time, $\tau = t$, the integrand is simply $\partial U/\partial y(t)$; at progressively earlier times the exponential term acts to multiply the velocity gradient by an ever-smaller factor.

Maxey (1978, 1982) proceeded to construct a turbulence model consisting of an algebraic relation between $-\overline{uv}/k$ and α_{eff} which was combined with α_{eff}- and k-equations together with a prescribed mixing length. The formulation is unconventional in terms of the familiar engineering turbulence models discussed in Section 2.1: since $-\overline{uv}$ is not linked explicitly to $\partial U/\partial y$ the model does not employ a turbulent viscosity (at least not in the straightforward manner indicated in Eq. (1)). In limited tests the model was applied to oscillatory channel flow and some qualitative comparisons with experimental data were reported. Mankbadi and Liu (1992) adopted Maxey's proposals in order to devise a second model, also for the calculation of periodically-oscillated wall-bounded flows. A triple decomposition of flow variables into mean (long-time-averaged), periodic, and turbulent quantities preceded the development of a closure for the periodic components (experimental data were used to prescribe all mean flow profiles). The model was intended for application to the high frequency, or 'quasi-laminar' (Finnicum and Hanratty, 1988), regime where the outer flow 'freezes' and the periodic variation is restricted to an increasingly narrow near-wall region as non-dimensionalized frequency is increased. Mankbadi and Liu's model relies upon a large number of simplifying assumptions, however, reasonable agreement with data was demonstrated for the intended range of application. Refinements of the model are presented by Brereton and Mankbadi (1993, 1995).

2.3. A strain parameter model

The original proposal of Townsend (1970) for an effective total strain equation incorporated advective and diffusive terms (but no destruction term). If, following Maxey, a sink term is included in order that the equation will retain the relaxation features discussed above, there follows an extension of Eq. (7) for application to inhomogeneous flows:

$$\frac{\mathrm{D}\alpha_{\text{eff}}}{\mathrm{D}t} = \frac{\partial U}{\partial y} + \frac{\partial}{\partial y}\left(\frac{\nu_t}{\sigma_\alpha}\frac{\partial \alpha_{\text{eff}}}{\partial y}\right) - \frac{\alpha_{\text{eff}}}{T_D}, \tag{10}$$

where σ_α is a turbulent Prandtl number for the diffusion of α_{eff}. Examination of Eq. (10) reveals that, in common with Eq. (7), it lacks a valid tensorial character (α_{eff} is a scalar, whereas $\partial U/\partial y$ is an element of a second rank tensor). It is taken as axiomatic in the development of modern turbulence closures that the only 'permissible' equations are those which conform to the constraints of tensor algebra (and hence are coordinate-independent; see Speziale, 1987, for example). Now, although present model applications are restricted to flows in simple shear, the complete model specification is to be developed from an expression of correct tensorial construction. Hence, replacing Eq. (10) let us write

$$\frac{\mathrm{D}S}{\mathrm{D}t} = T_D\left(2\Sigma_{ij}\,\Sigma_{ij}\right) + \frac{\partial}{\partial x_j}\left(\frac{\nu_t}{\sigma_s}\frac{\partial S}{\partial x_j}\right) - \frac{S}{T_D}. \tag{11}$$

S is termed a 'strain parameter', Σ_{ij} is the strain rate tensor, $\Sigma_{ij} = \frac{1}{2}(\partial U_i/\partial x_j + \partial U_j/\partial x_i)$, and σ_s is a turbulent Prandtl number for diffusion of S. Note that the source term is specified as $T_D(2\Sigma_{ij}\Sigma_{ij})$, in preference to $(2\Sigma_{ij}\Sigma_{ij})^{1/2}$ which would follow more directly from Eq. (10): the adoption of the former expression was guided by a preliminary study in which it was found that the effective use of $|\partial U/\partial y|$ implied by the second form could give rise to unphysical flow profiles. The more fundamental decision to select the strain rate tensor is considered further below. In application to homogeneous flows the S-equation reduces to

$$\frac{\partial S}{\partial t} = T_D\left(\frac{\partial U}{\partial y}\right)^2 - \frac{S}{T_D}. \tag{12}$$

The behaviour of Eq. (12) may be compared with that of Eq. (7): if T_D and $\partial U/\partial y$ are taken to be constant and the initial condition is $S=0$ at $t=0$, the solution of the equation (cf. Eq. (8)) is obtained as

$$S = \left(T_D\frac{\partial U}{\partial y}\right)^2 [1 - \exp(-t/T_D)]. \tag{13}$$

The short-time ($t \ll T_D$) and long-time ($t \gg T_D$) approximations to Eq. (13) are respectively

$$S = \left(t\frac{\partial U}{\partial y}\right)\left(T_D\frac{\partial U}{\partial y}\right) \tag{14}$$

and

$$S = \left(T_D\frac{\partial U}{\partial y}\right)^2. \tag{15}$$

Eq. (14) shows S to be a form of modified total strain in which the total strain $t\cdot\partial U/\partial y$ is multiplied by the group $T_D\cdot\partial U/\partial y$. The long-time asymptote, Eq. (15), gives S simply as the square of total strain truncated on T_D.

Observing that the leading term on the right of Eq. (11) reduces to $T_D(\partial U/\partial y)^2$ for any flow in simple shear, the specification of the square of the strain rate tensor is seen to be arbitrary. In other words, constructions involving the vorticity tensor, $\Omega_{ij} = \frac{1}{2}(\partial U_i/\partial x_j - \partial U_j/\partial x_i)$, such as $\Omega_{ij}\Omega_{ij}$, $\Omega_{ij}\Sigma_{ij}$, or some other form might equally be selected. The final choice within the ad hoc framework pursued here must largely be determined by optimization against data for complex flows. (It is interesting to note the recent appearance in the literature of two related, but independent, works adopting similarly ad hoc approaches: Lumley et al. (1996), in relation to dissipation rate modelling, consider an equation for an inverse timescale where the source term is of the form $(\Sigma_{ij}\Sigma_{ij})^{1/2}$; Spalart and Allmaras (1994) devise an equation for the transport of turbulent viscosity and employ $(\Omega_{ij}\Omega_{ij})^{1/2}$.)

It now remains to complete the specification of a closed k–ϵ–S turbulent viscosity model. The present study has focused essentially upon the constitutive equation and the S-transport equation; the remaining model elements have been taken almost directly from the Launder and Sharma (1974) k–ϵ closure. Retaining the most general form of the model expressed in Cartesian tensor notation, the full equation set reads

$$-\overline{u_i u_j} = \nu_t\left(\frac{\partial U_i}{\partial x_j} + \frac{\partial U_j}{\partial x_i}\right) - \frac{2}{3}\,\delta_{ij}k, \tag{16}$$

$$\nu_t = C_\mu f_\mu(\mathrm{Re}_t) f_S(S)\,\frac{k^2}{\tilde{\epsilon}}, \tag{17}$$

$$f_S(S) = \frac{2.88}{1 + 0.165S}\left(1 - 0.55\,\exp\left[-\left(0.135S + 0.0015S^3\right)\right]\right), \tag{18}$$

$$f_\mu(\mathrm{Re}_t) = 1 - 0.3\,\exp\left[-0.02\,\mathrm{Re}_t\right], \quad \mathrm{Re}_t = \frac{k^2}{\nu\tilde{\epsilon}}, \tag{19}$$

$$\frac{\mathrm{D}k}{\mathrm{D}t} = \nu_t\left(\frac{\partial U_i}{\partial x_j} + \frac{\partial U_j}{\partial x_j}\right)\frac{\partial U_i}{\partial x_j} + \frac{\partial}{\partial x_j}\left(\left(\nu + \frac{\nu_t}{\sigma_k}\right)\frac{\partial k}{\partial x_j}\right) - \left(\tilde{\epsilon} + D_\epsilon\right), \tag{20}$$

where

$$D_\epsilon = 2\nu\left(\partial k^{1/2}/\partial x_j\right)^2,$$

$$\frac{\mathrm{D}\tilde{\epsilon}}{\mathrm{D}t} = C_{\epsilon 1}\,\frac{\tilde{\epsilon}}{k}\,\nu_t\left(\frac{\partial U_i}{\partial x_j} + \frac{\partial U_j}{\partial x_i}\right)\frac{\partial U_i}{\partial x_j} + \frac{\partial}{\partial x_j}\left(\left(\nu + \frac{\nu_t}{\sigma_\epsilon}\right)\frac{\partial\tilde{\epsilon}}{\partial x_j}\right) - C_{\epsilon 2}\,\frac{\tilde{\epsilon}^2}{k} + 0.9\,\nu\,\nu_t\left(\frac{\partial^2 U_j}{\partial x_k \partial x_l}\right)^2, \tag{21}$$

$$\frac{\mathrm{D}S}{\mathrm{D}t} = \frac{1}{2}\,\frac{k}{\tilde{\epsilon}}\left(\frac{\partial U_i}{\partial x_j} + \frac{\partial U_j}{\partial x_i}\right)^2 + \frac{\partial}{\partial x_j}\left(\frac{\nu_t}{\sigma_S}\frac{\partial S}{\partial x_j}\right) - \frac{S}{(k/\tilde{\epsilon})}, \tag{22}$$

where

$C_\mu = 0.09$; $\sigma_k = 1.0$; $\sigma_\epsilon = 1.21$; $\sigma_S = 6.0$;
$C_{\epsilon 1} = 1.44$; $C_{\epsilon 2} = 1.92$.

The constitutive relation, Eq. (16), is of the standard form in the sense that the prescription of the Reynolds stress in relation to the mean strain rate includes only linear velocity gradient elements. (Non-linearities do arise from the damping function which acts upon the local strain parameter.)

Support for the form of the leading term in the expression for $f_S(S)$, Eq. (18), is supplied from two different sources in relation to 'long-time' conditions (i.e. where Eq. (15) applies and $T_D = k/\epsilon$, discussed further below). Firstly we might follow Launder's (1986) analysis of Reynolds stress transport models. Launder showed that in the absence of convection and diffusion, the Reynolds stress model of Gibson and Launder (1978) applied to fully-developed wall-bounded flow yields $-\overline{uv} = c\left(\overline{v^2}/k\right)(k^2/\epsilon)\partial U/\partial y$. If the analysis is extended to eliminate $\overline{v^2}/k$ using the equations of the Reynolds stress model then we obtain $-\overline{uv} = [a/(1+bS)]\,(k^2/\epsilon)\partial U/\partial y$ in accordance with Eqs. (16)–(18). The second strand of support comes from the work of Hunt and Maxey (1978) who advanced a corresponding form based upon homogeneous flow calculations (see also Mankbadi and Liu, 1992). The exponential multiplier in Eq. (18) acts to limit values of f_S at low S. The complete expression for f_S gives $f_S = 1.0$ at $S = C_\mu^{-1}$. Thus, under such equilibrium conditions and at sufficiently high Re_t, the standard high-Reynolds-number expression for ν_t (Eq. (2)) is recovered from Eq. (17).

Turning next to the specification of $f_\mu(\mathrm{Re}_t)$, it is to be recalled from the discussion of Section 2.1 that such a viscous damping function should ideally be restricted to regions of

low turbulent Reynolds number. This requirement is, in fact, met by Eq. (19): for example $f_\mu = 0.9$ at $\mathrm{Re_t} = 50$ (corresponding to $y^+ \simeq 7$ in a wall-bounded flow). It should be noted that, following the LS model, ϵ is replaced by $\tilde{\epsilon}$ in the definition of $\mathrm{Re_t}$ and throughout the present model.

In relation to the transport equations of the model, it is first seen that the k-equation, Eq. (20), is completely unaltered from the form adopted in the LS model. The ϵ-equation is re-tuned in three respects: the turbulent Prandtl number for ϵ-diffusion is set to 1.21 ($\sigma_\epsilon = 1.3$ in the LS model), no function is included in the third term on the right of Eq. (21) (in the LS model $C_{\epsilon 2}$ is multiplied by $f_2 = 1 - 0.3\ \exp(-\mathrm{Re_t}^2)$), and the coefficient of final term is taken as 0.9 (2.0 in the LS model). In the equation for the strain parameter T_D is set equal to the large-scale turbulence timescale, $k/\tilde{\epsilon}$ (compare Eq. (22) with Eq. (11)). Viscous diffusion is omitted from the S-equation: the strain parameter is not a dynamical quantity and there is no analogy with the molecular transport of momentum that gives rise to the viscous terms of the Navier–Stokes equations. The large value of σ_S was selected in order to limit the influence of turbulent diffusion in the S-equation.

Some further aspects of the strain parameter model, and in particular its relationship to Rapid Distortion Theory, are discussed at greater length in a report by the present authors (Cotton and Ismael, 1996).

3. Results

Results are presented below for unsteady homogeneous flows, steady fully-developed channel flow, and mixed convection pipe flows. The model constants and functions detailed in Section 2.3 were assigned by reference to the wall-bounded flows, subsequent examination against data for homogeneous shear flows being undertaken in a completely 'unseen' trial. In the present section, however, results are presented first for homogeneous flows in view of their relative simplicity and also because of their direct correspondence to the discussion above.

3.1. Homogeneous flow results

In a homogeneous flow single point ensemble averages are uniform in space and therefore advective and diffusive terms are absent from the ensemble-averaged governing equations. If a constant and uniform strain rate, $\partial U/\partial y$ is applied at $t = 0$, Eqs. (16), (20)–(22) for the determination of the Reynolds stress, $-\overline{uv}$, turbulent kinetic energy, dissipation rate, and strain parameter read

$$-\overline{uv} = \nu_\mathrm{t}\,\frac{\partial U}{\partial y}, \tag{23}$$

$$\frac{\partial k}{\partial t} = -\overline{uv}\,\frac{\partial U}{\partial y} - \epsilon, \tag{24}$$

$$\frac{\partial \epsilon}{\partial t} = C_{\epsilon 1}\,\frac{\epsilon}{k}\,(-\overline{uv})\,\frac{\partial U}{\partial y} - C_{\epsilon 2}\,\frac{\epsilon^2}{k}, \tag{25}$$

$$\frac{\partial S}{\partial t} = \frac{k}{\epsilon}\left(\frac{\partial U}{\partial y}\right)^2 - \frac{S}{(k/\epsilon)}. \tag{26}$$

Note that ϵ and $\tilde{\epsilon}$ are identical and that the final term of Eq. (21) is omitted in writing Eq. (25). ν_t is determined from Eqs. (17)–(19). Numerical solution of the (non-dimensionalized) turbulence model equations is obtained using the Runge–Kutta procedures of the 'MATLAB' software package.

Comparison is made first with the windtunnel measurements of Tavoularis and Corrsin (1981). The windtunnel was divided into a series of channels of varying flow resistance in order to obtain a uniform strain rate. An array of rods downstream of the channels was used to generate turbulence which developed with approximately homogeneous properties in planes normal to the direction of flow. The spatial development of the flow in the streamwise direction therefore corresponds to the temporal development of a 'true' homogeneous flow. In Eqs. (24)–(26) the differential operator $\partial/\partial t$ is replaced by $U_c\partial/\partial x$, where U_c is the mean flow velocity at the mid-section of the windtunnel. Dimensionless time, t^*, is defined as $t^* = (x/U_c)\ \partial U/\partial y$, and results are shown below for $t^* \geqslant 8.6$ (from which time Tavoularis and Corrsin present tabulated data). The measured dimensionless strain rate of these experiments, $(k/\epsilon)\ \partial U/\partial y$, shows a small variation from 6.5 to 6.1 over the length of the test section.

The experiments of Tavoularis and Corrsin were conducted at high Reynolds number, $\mathrm{Re_t} \gtrsim 2000$, and therefore $f_\mu(\mathrm{Re_t})$ is set to unity in Eq. (17). In consequence, the only differences between the present model and the standard high-Reynolds-number k–ϵ model of Launder and Spalding (1974) lie in the current inclusion of $f_s(S)$, Eq. (18), as an element of the constitutive equation, and the determination of S from solution of Eq. (26). Fig. 1(a)–(c) show the development of $-\overline{uv}/k$, k/k_0, and ϵ/ϵ_0, as measured by Tavoularis and Corrsin and computed using the present model, standard high-Reynolds-number k–ϵ model, and a modified k–ϵ model. The subscript 0 here denotes conditions at the start of a computed simulation. The experimental data for $-\overline{uv}/k$ shown in Fig. 1(a) indicate that the structural ratio is essentially constant over the period (or distance) considered. The present model is in good agreement with the data, although the calculations indicate a slow decrease with time that is not apparent in the measurements. The standard k–ϵ model returns values of $-\overline{uv}/k$ which are considerably higher than the measured values. A simple modification to the k–ϵ model is also examined in Fig. 1(a): in these calculations C_μ is halved to 0.045, all other aspects of the standard model being unchanged. The modification produces much closer agreement with data than does the standard model (in an earlier work Speziale and Mac Giolla Mhuiris (1989) altered C_μ to 0.055 in making comparison with the data of Tavoularis and Corrsin). The development of turbulent kinetic energy shown in Fig. 1(b) reveals the present model to be in close agreement with data; the standard model is far too energetic, and the 'modified standard' model produces values of k/k_0 only slightly greater than those of the data. Results for the growth of the dissipation rate, Fig. 1(c), show broadly similar behaviour, however, it is now the modified k–ϵ model that is in best agreement with data. The present model slightly underpredicts levels of ϵ/ϵ_0 and this is reflected in the variation of $(k/\epsilon)\partial U/\partial y$ which is calculated to increase from 6.5 to 7.1 over the range $t^* = 8.6$–13.0 (cf. the measured values above). S, which is related to $(k/\epsilon)\partial U/\partial y$ via Eq. (26), is calculated to increase from 30.3 to 38.0. The performance of the present model in simulating Tavoularis and Corrsin's experiments (and those of Lee et al. below) is attributable to two factors: firstly, the introduction of an additional 'degree of freedom' in the form of the strain parameter allows the initial state $-(\overline{uv}/k)_0$ to be matched to data; secondly, the accurate performance of the model at later times indicates that appropriate values of $f_s(S)$ are generated by the equation set. In order to achieve comparable accuracy using a high-Reynolds-number k–ϵ model, the value of C_μ has been tuned on a trial-and-error basis (and halved in this case).

The study of Abe et al. (1997) includes a comparison with the data of Tavoularis and Corrsin that is particularly pertinent to the present modelling approach. Abe et al. advanced a refinement of the Speziale (1987) non-linear turbulent viscosity model using concepts associated with Reynolds stress trans-

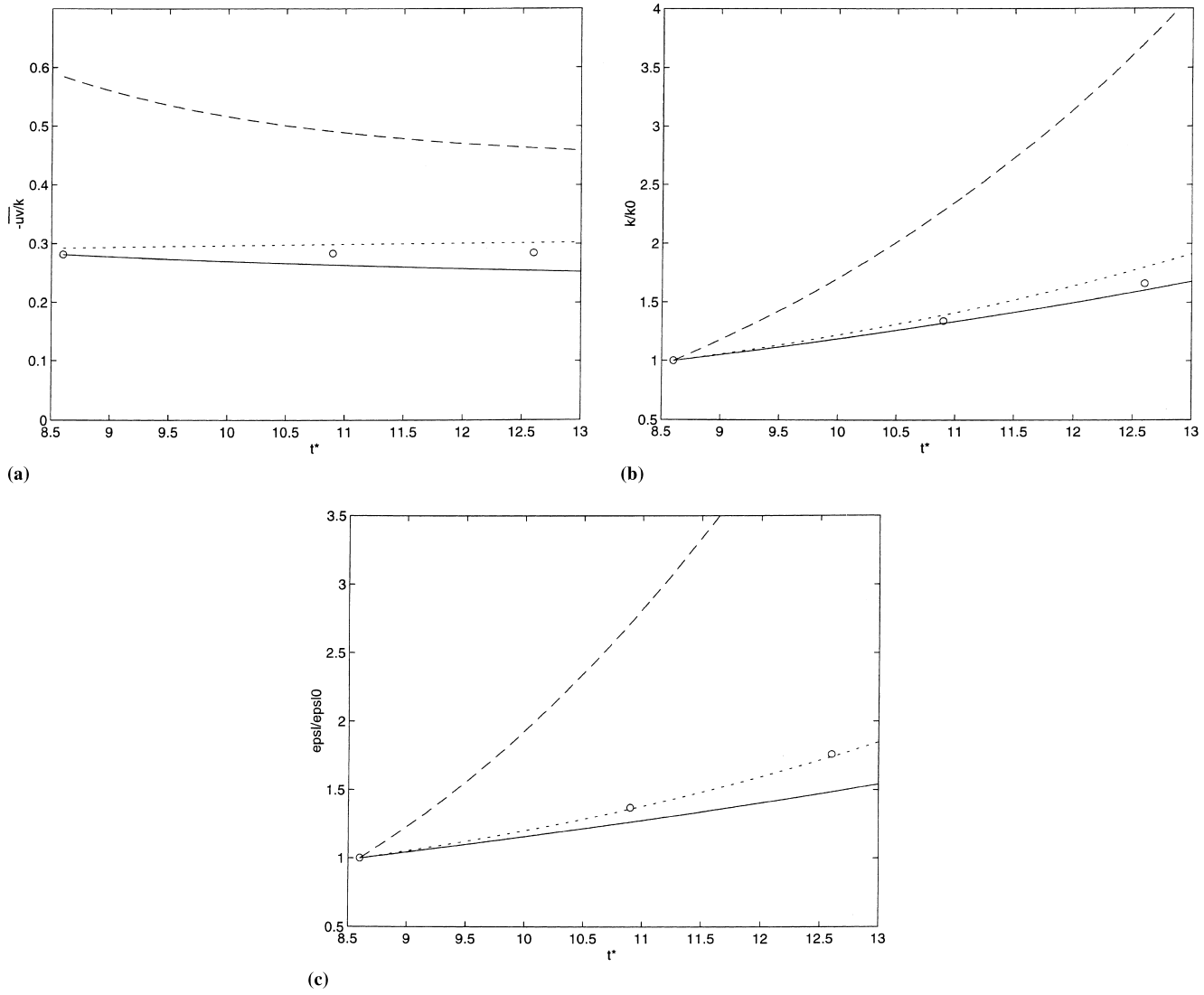

Fig. 1. Homogeneous flow development at low dimensionless strain rate. (a) $-\overline{uv}/k$; (b) k/k_0; (c) ϵ/ϵ_0. ○ Experimental data of Tavoularis and Corrsin (1981); ——— present model; - - - standard k–ϵ model; ····· k–ϵ model with $C_\mu = 0.045$.

port models. Applied to the calculation of $-\overline{uv}$ in homogeneous flow, the refined model incorporates a damping term that is dependent on $[(k/\epsilon)\partial U/\partial y]^2$. Abe et al. were able to show that their approach led to a clear improvement in the calculation of Tavoularis and Corrsin's data.

The second set of homogeneous flow data to be considered is that of Lee et al. (1987) who generated DNS results for a temporally-unsteady and spatially-homogeneous flow. Dimensionless time, t^* is now equal to the total strain, $t^* = t\cdot\partial U/\partial y$. Comparison is made with the results of Lee et al. for $t^* \geqslant 4$. The DNS data used in the comparisons below are for a high dimensionless strain rate: Lee et al. calculated that $(k/\epsilon)\partial U/\partial y$ rises from 21.6 to 35.0 over the course of the transient, giving values that are approximately 3–6 times larger than the strain rates characterizing the experimental data of Tavoularis and Corrsin (1981). The DNS data were generated for an extremely low Reynolds number flow, $\mathrm{Re}_t \simeq 10$ at $t^* = 4$, and the present model is now applied with the function $f_\mu(\mathrm{Re}_t)$ as given by Eq. (19) included in Eq. (17). The standard k–ϵ model is extended to low-Reynolds-number form by inclusion of the Launder and Sharma (1974) damping function:

$$f_\mu = \exp\left[\frac{-3.4}{(1 + Re_t/50)^2}\right]. \tag{27}$$

Flow development calculated using the present model and the LS model is shown in Fig. 2(a)–(c) together with the DNS data of Lee et al. The direct simulation data for $-\overline{uv}/k$ show that the ratio decays over the time interval considered; the behaviour is captured well by the present model, whereas the LS model erroneously indicates increasing $-\overline{uv}/k$. Turbulent kinetic energy development shown in Fig. 2(b) indicates that the present model returns values of k/k_0 that are somewhat low, however the LS model shows a rate of growth of k that is far too high. In Fig. 2(c) it is seen that both models yield excessive rates of increase of ϵ/ϵ_0 (with the performance of the LS model being considerably worse than that of the present model). It should, however, be recalled that effort in the development of the strain parameter closure has been concentrated upon model elements other than the ϵ-equation, and it is well-known that the equation suffers significant weaknesses, see for example Rodi and Mansour (1990). The inaccurate computation of the dissipation rate again affects the variation

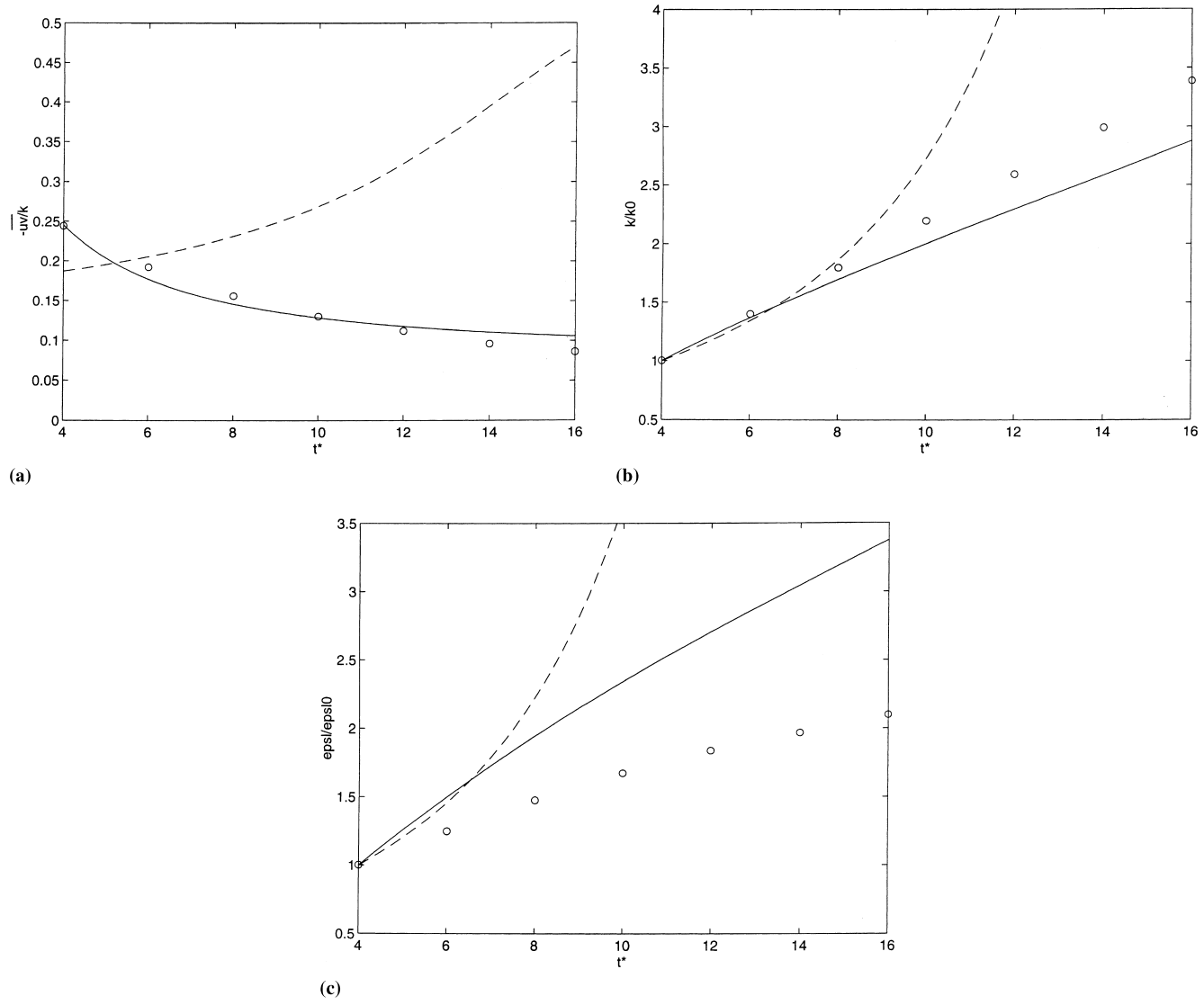

Fig. 2. Homogeneous flow development at high dimensionless strain rate: inclusion of viscous influences. (a) $-\overline{uv}/k$; (b) k/k_0; (c) ϵ/ϵ_0. ○ DNS data of Lee et al. (1987); ——— present model; - - - LS model.

of $(k/\epsilon)\partial U/\partial y$ which is now calculated using the present model to decrease from 21.6 at the start of the transient to 18.4 at $t^* = 16$; over the same interval S increases from 98.5 to 217.9.

3.2. Channel flow results

The next data to be considered are the fully-developed channel flow DNS results of Kim et al. (1987) and Kim (1990) (communicated to Rodi and Mansour, 1990 and Michelassi et al., 1991). The DNS data of Kim et al. were generated for a low Reynolds number flow: $\mathrm{Re}_\tau = U_\tau H/\nu = 180$; the corresponding bulk Reynolds number, $\mathrm{Re} = 2U_\mathrm{b}H/\nu$, is equal to 5600. Kim (1990) employed a higher Reynolds number, $\mathrm{Re}_\tau = 395$, or $\mathrm{Re} = 13750$. The constants and functions of the present model were tuned by reference to isothermal channel and heated mixed convection flows, and the results presented below should therefore be viewed as those of a (partial) optimization of a generic model formulation. Eqs. (16)–(22) now apply, although in the fully-developed condition the only non-zero strain rate is $\partial U/\partial y$. The wall boundary conditions on k and $\tilde{\epsilon}$ are $k = \tilde{\epsilon} = 0$ (Jones and Launder, 1972). A near wall asymptotic analysis of Eq. (22) (with $k \sim y^2$ and $\tilde{\epsilon} \sim y$ in order to balance Eqs. (20) and (21) to lowest order) indicates that $S \sim y^2$ and consequently the wall boundary condition $S = 0$ is applied. The turbulence model equations are solved in conjunction with the momentum and continuity equations:

$$\frac{\mathrm{D}(\rho U)}{\mathrm{D}t} = -\frac{\mathrm{d}p}{\mathrm{d}x} + \frac{\partial}{\partial y}\left[(\mu + \mu_\mathrm{t})\,\frac{\partial U}{\partial y}\right], \tag{28}$$

$$\frac{\partial U}{\partial x} + \frac{\partial V}{\partial y} = 0. \tag{29}$$

The zero gradient boundary condition is applied to all variables at the channel axis (except that $V = 0$). Numerical solution of the governing equations is obtained using a finite volume/finite difference method adapted from the parabolic scheme of Leschziner (1982). An expanding grid of 100 control volumes is employed and the wall-adjacent node is positioned at $y^+ \simeq 0.25$. The solution is started from approximate flow profiles and is marched in the streamwise direction until a fully-developed condition is attained.

Comparison is made first with a correlation for local friction coefficient proposed by Dean (1978):

$$c_f = \frac{\tau_w}{(1/2)\rho U_b^2} = 0.073\ \mathrm{Re}^{-0.25}. \quad (30)$$

Values of c_f returned by the present and LS models at Re $= 5600$ are 7.7×10^{-3} and 7.3×10^{-3}, respectively. These values represent discrepancies of -8% and -13% with respect to Eq. (30). The local friction coefficient obtained by Lee et al. was 8.2×10^{-3}, a value 2% lower than Dean's correlation. Dean noted that the experimental data to which Eq. (30) was fitted showed some scatter (and also the equation is strictly applicable only for Re > 6000). Thus, although the present value of c_f is somewhat lower than that calculated by Kim et al. and the value returned by Eq. (30), it does appear to be more accurate than the LS value. At the higher Reynolds number of 13750 the present and LS models respectively calculate c_f to be 6.3×10^{-3} and 5.8×10^{-3} (-6% and -13% with respect to Dean's correlation).

Turning next to the DNS flow profile data of Kim et al. (1987) for $\mathrm{Re}_\tau = 180$ and the data of Kim (1990) for $\mathrm{Re}_\tau = 395$, Fig. 3(a) and (b) show velocity profiles (with $U^+ = U/U_\tau$) computed using the present and LS models together with the DNS data. Also shown is the 'law of the wall' where the constants in the semi-logarithmic expression are those specified by Patel and Head (1969):

$$U^+ = y^+, \quad (31)$$

$$U^+ = 5.45 + 5.5\ \log_{10} y^+. \quad (32)$$

At both Reynolds numbers the present model is in better agreement with the DNS data than is the LS model. The vertical displacements of the velocity profiles are consistent with the results for local friction coefficient discussed above.

Reynolds stress $\left(-\overline{uv}^+ = -\overline{uv}/U_\tau^2\right)$ and turbulent kinetic energy ($k^+ = k/U_\tau^2$) profiles are shown in Figs. 4 and 5. The present model is again considerably closer than the LS model to the DNS data, and the improved resolution of the near-wall peak in turbulent kinetic energy is particularly noticeable. Profiles of the dissipation rate ($\epsilon^+ = \epsilon\nu/U_\tau^4$) are shown in Fig. 6 (the DNS data for $\mathrm{Re}_\tau = 180$ are those of Mansour et al., 1988, derived from the same database as the results of Lee et al.). The present model is accurate for $y^+ \geqslant 30$, and shows an improvement over the LS model in the wall-adjacent region. The fact that neither model is highly accurate near the wall again reflects the highly approximate nature of the ϵ-equation.

Distributions of the damping function, f are shown in Fig. 7(a) and (b). In the present model $f = f_\mu f_s$, Eqs. (18) and (19); in the LS model $f = f_\mu$, Eq. (27). As noted in Section 2.3, the present expression for $f_\mu(\mathrm{Re_t})$ rapidly asymptotes towards unity (from a value of 0.7 at the wall). The variation of the composite damping function is therefore almost entirely associated with the contribution of $f_s(S)$. Comparison with DNS data for $\mathrm{Re}_\tau = 180$, Fig. 7(a), shows the present model to be considerably closer to the data than the LS model. The present model returns values of f somewhat lower than the DNS values for $y^+ \geqslant 40$; it does, however, correctly show that f exceeds unity away from the wall at the low bulk Reynolds number of this case. The higher Reynolds number case, $\mathrm{Re}_\tau = 395$, Fig. 7(b), shows the present model to be in excellent agreement with DNS data, although it should be noted that particular emphasis was placed upon these data in the process of tuning the model parameters.

Further examination of Fig. 7(a) and (b) yields information on bulk Reynolds number effects. It is seen from the DNS data that the increase in Reynolds number from Fig. 7(a) to

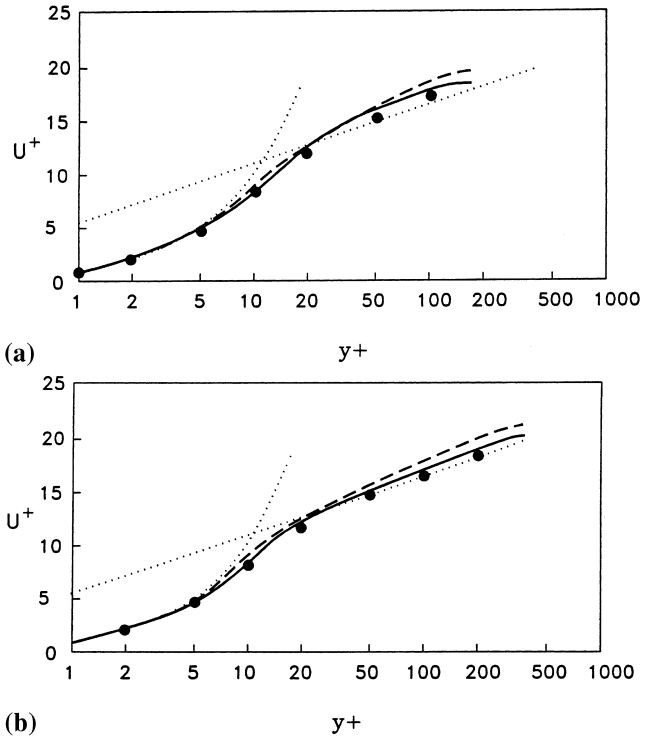

Fig. 3. Velocity profiles in channel flow. (a) $\mathrm{Re}_\tau = 180$ (Re = 5600); (b) $\mathrm{Re}_\tau = 395$ (Re = 13750). ● DNS data of Kim et al. (1987) and of Kim (1990); ——— present model; - - - LS model, ····· Eqs. (31) and (32).

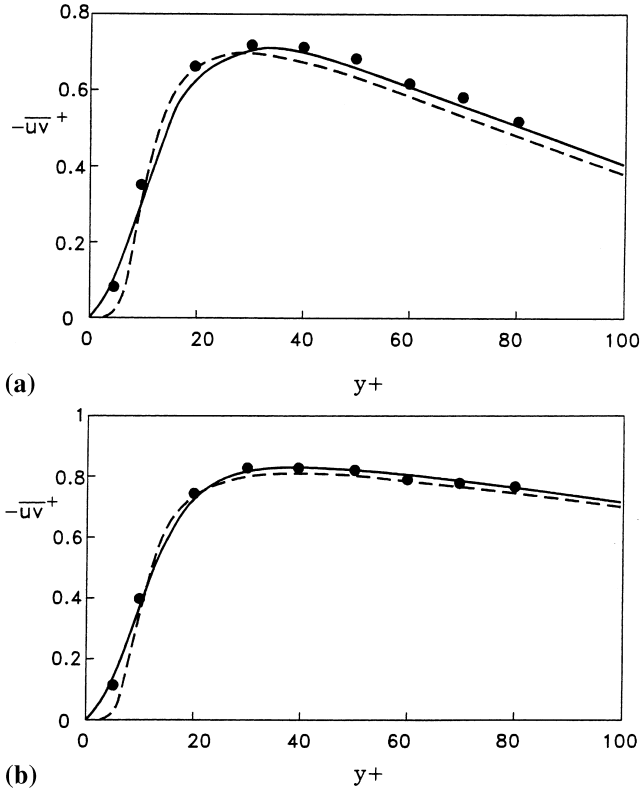

Fig. 4. Reynolds stress profiles in channel flow. (a) $\mathrm{Re}_\tau = 180$; (b) $\mathrm{Re}_\tau = 395$. ● DNS data of Kim et al. (1987) and of Kim (1990); ——— present model; - - - LS model.

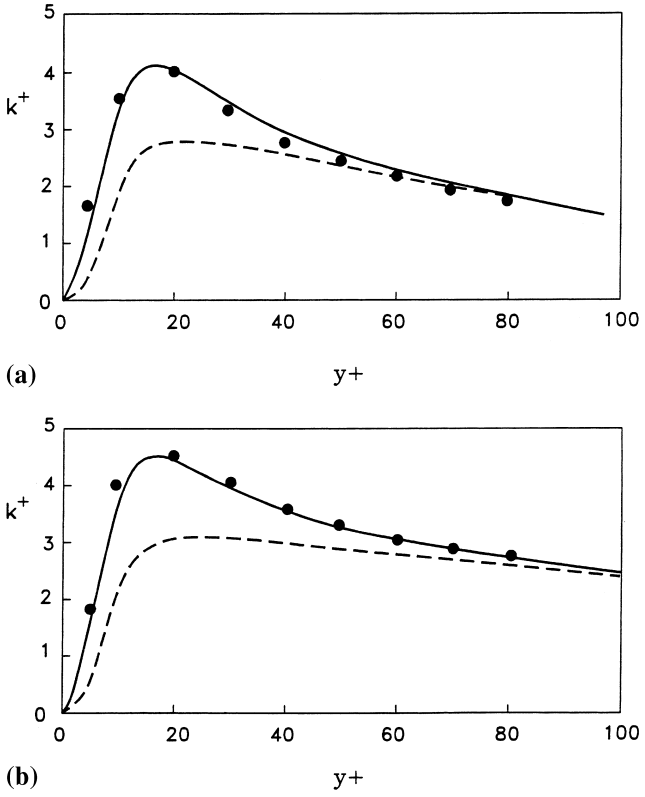

Fig. 5. Turbulent kinetic energy profiles in channel flow. (a) $Re_\tau = 180$; (b) $Re_\tau = 395$. ● DNS data of Kim et al. (1987) and of Kim (1990); ——— present model; - - - LS model.

Fig. 7(b) is accompanied by a *decrease* in the level of the damping function. This trend is also clear in the present results, at least for $y^+ \geqslant 40$. Such behaviour cannot, however, be resolved by a model with damping dependent solely upon turbulent Reynolds number: Re_t at given y^+ increases with bulk Reynolds number, and assuming that $f = f_\mu(Re_t)$ is an increasing function, it follows that f at given y^+ also *increases* with bulk Reynolds number.

3.3. Mixed convection results

The regime of 'mixed' convection is said to occur in heated flows where a forced convection (pressure gradient driven) flow is significantly modified by the action of buoyancy. Present interest is centred on vertical uniformly-heated pipe flows: mixed convection conditions in such flows arise where the Reynolds number ($Re = U_b D/\nu$) is relatively low and the Grashof number relatively high. In the case of ascending pipe flow, the principal effect of practical importance relates to a part of the mixed convection region over which there occurs a reduction in heat transfer levels (i.e. heat transfer coefficient or Nusselt number) to below 50% of the corresponding forced convection value. Experimental and computational investigations of mixed convection are reviewed by Petukhov and Polyakov (1988) and Jackson et al. (1989). The latter authors quote a 'buoyancy parameter', Bo (originally developed by Hall and Jackson, 1969) to characterize the extent of mixed convection influences:

$$Bo = \frac{Gr}{Re^{3.425} Pr^{0.8}}. \tag{33}$$

Variable property effects other than those associated with buoyancy become significant where the temperature variations in a flow are large. An appropriate dimensionless measure of temperature variation is provided by the 'heat loading parameter', q^+ (see for example Vilemas et al., 1992):

$$q^+ = \frac{\dot{q}}{\rho U_b c_p \theta}. \tag{34}$$

In the present computations the k–ϵ–S and LS turbulence models are solved together with the continuity equation, the momentum equation (including the body force term, $-\rho g$), and the energy equation (in which turbulent Prandtl number is set to 0.9). All equations are written in full variable properties form following Cotton and Kirwin (1995). Direct buoyant production terms are omitted from the turbulence model equations (an approximation examined by Cotton and Jackson, 1990). The numerical procedures are based upon the same finite volume/finite difference scheme as that used for the channel flow calculations above. Full details of the governing mean flow equations and the solution methodology are provided by Kirwin (1995).

In the course of the present programme of research comparison was made with over 20 individual experimental test cases. Here, in the interests of brevity, the results shown are restricted to two carefully selected ascending air flow cases of Vilemas et al. (1992), as supplemented by the additional data of Poškas (1991). The data are selected in two senses: firstly, the two experimental runs were obtained for similar values of Bo, but widely different values of q^+; secondly, the first test case below represents the *worst* performance of the present model amongst all the test cases considered.

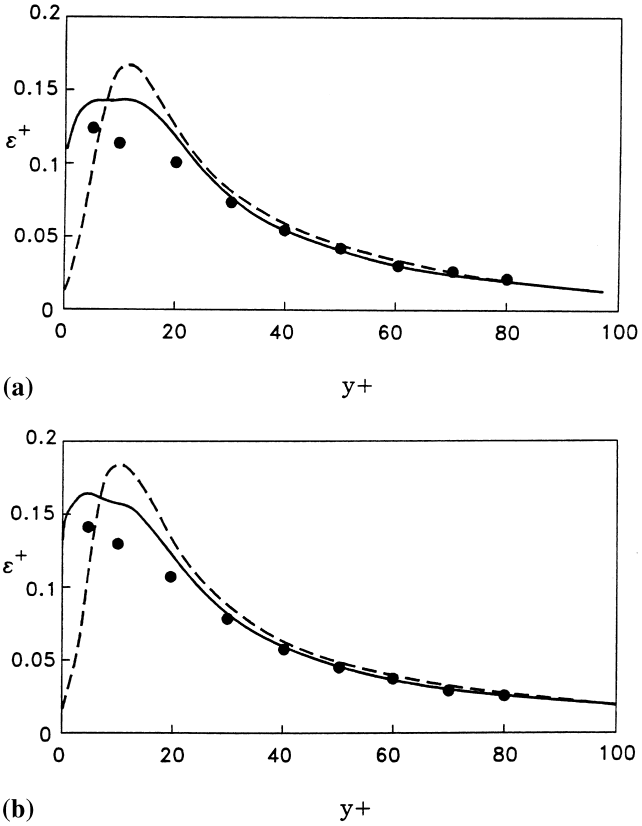

Fig. 6. Dissipation rate profiles in channel flow. (a) $Re_\tau = 180$; (b) $Re_\tau = 395$. ● DNS data of Mansour et al. (1988) and of Kim (1990); ——— present model; - - - LS model.

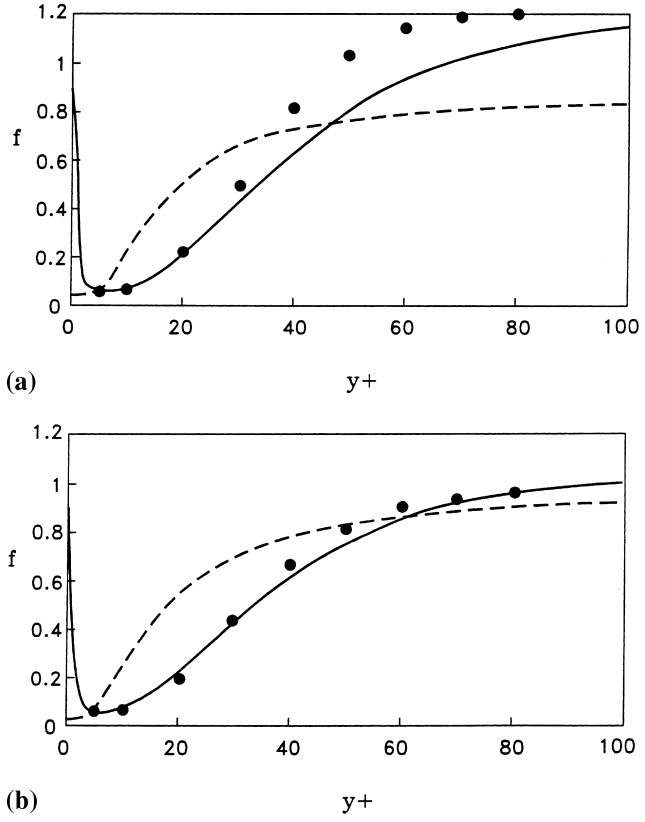

Fig. 7. Damping function profiles in channel flow. (a) $Re_\tau = 180$; (b) $Re_\tau = 395$. ● DNS data of Kim et al. (1987) and of Kim (1990); ——— present model; - - - LS model.

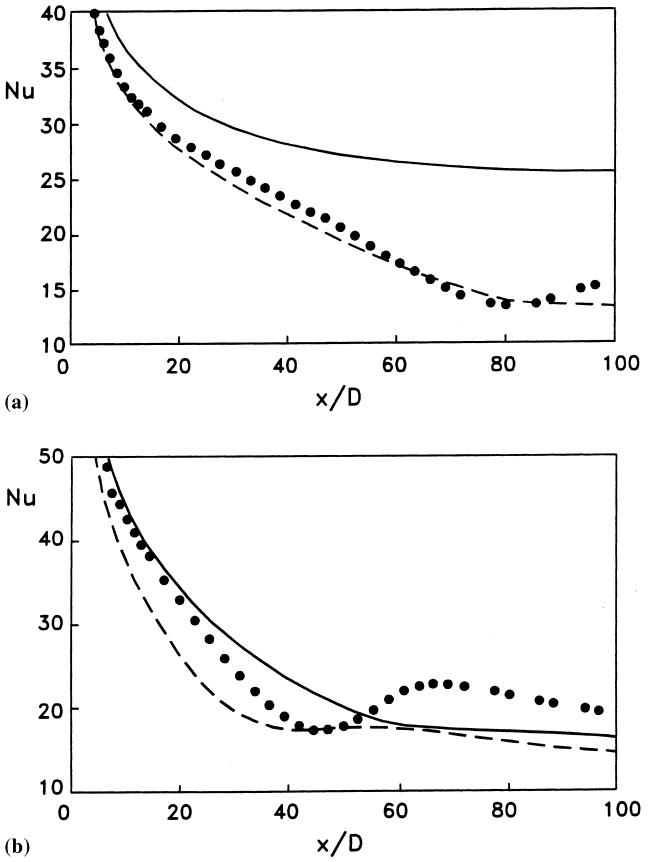

Fig. 8. Nusselt number developing in ascending mixed convection air flow. (a) $Re = 1.33 \times 10^4$, $Gr = 2.41 \times 10^8$; (b) $Re = 1.96 \times 10^4$, $Gr = 1.21 \times 10^9$. ● Data of Vilemas et al. (1992); ——— present model; - - - LS model.

The Nusselt number data shown in Fig. 8(a) were obtained for $Re = 1.33 \times 10^4$, $Pr = 0.71$, and $Gr = 2.41 \times 10^8$ at the start of heating (corresponding to $Bo = 2.4 \times 10^{-6}$ and $q^+ = 3.0 \times 10^{-4}$). Results obtained using the present and LS models are also shown and it is apparent that, for this case at least, the LS model is in much closer agreement with data. The case is, however, exceptional, and is included here for the sake of completeness in presenting results generated using a new turbulence model.

The data shown in Fig. 8(b) were generated with initial conditions $Re = 1.96 \times 10^4$, $Pr = 0.71$, and $Gr = 1.21 \times 10^9$ ($Bo = 3.2 \times 10^{-6}$ and $q^+ = 9.5 \times 10^{-4}$). Thus, the two sets of measurements were obtained for similar values of the buoyancy parameter (characteristic of significantly reduced heat transfer levels: constant property forced convection Nusselt numbers at the Reynolds numbers of the tests might be expected to lie in the range Nu ≈35–50, cf. values as low as 15–20 in Fig. 8(a) and (b)). The two cases are distinguished, however, in terms of the heat loading parameter, variable property effects being considerably more significant in Fig. 8(b). It is seen that the two turbulence models perform comparably against the data of Fig. 8(b), a result that is far more representative of the complete mixed convection test series (full details are available from the authors). Notwithstanding this last remark, it is the case that scope remains for further tuning of the present model.

4. Concluding remarks

The physical grounds for the inclusion of a strain parameter, S as an element of a relatively simple (3-equation) turbulence model were presented in Section 2. Modification of the stress/rate-of-strain relation in the model from its 'high-Reynolds-number' form occurs primarily in response to variations in S, with only limited dependence on the turbulent Reynolds number, Re_t.

In application to homogeneous flows, the model has been compared against the experimental data of Tavoularis and Corrsin (1981) and the DNS results of Lee et al. (1987). Close agreement is obtained with the lower strain rate case of Tavoularis and Corrsin; while there are some discrepancies with respect to the 'rapid' case of Lee et al., it is demonstrated nonetheless that the new model can resolve the temporal development of homogeneous flows with considerably greater accuracy than k–ϵ schemes. The k–ϵ–S model is seen to reproduce the DNS channel flow data of Kim et al. (1987) and Kim (1990) more closely than does the widely-used low-Reynolds-number k–ϵ model of Launder and Sharma (1974). (It should, however, be noted that channel flows were the most important 'target' data in tuning the constants and functions of the present model.) Particularly noticeable is the ability of the k–ϵ–S model to resolve Reynolds number effects apparent in the DNS data for the damping function. In relation to buoyancy-influenced, or mixed convection flows, while the full set of model runs undertaken show the performance returned by the present model to be similar to that of the Launder and Sharma model, an isolated 'unfavourable' case has been included in Section 3. Work continues to evaluate the k–ϵ–S and alternative strain-parameter-based methodologies.

Acknowledgements

The work presented here was supported by the Engineering and Physical Sciences Research Council and the Defence Evaluation and Research Agency (Grant GR/H74247). Different aspects of the study, 'Turbulence model development with reference to strain rate, vorticity, and the turbulence timescales', were undertaken by staff at the University of Manchester and UMIST, and we are pleased to acknowledge our discussions with Professor B.E. Launder, Dr. T.J. Craft and Dr. K. Suga. Additional calculations for the channel flow cases were undertaken by Mr. C. Blundell, and Dr. P.J. Kirwin supplied the computer code used as the basis for the mixed convection calculations. Some of the results shown here were presented in preliminary form at the 1994 International Symposium on Turbulence, Heat and Mass Transfer and the 10th Symposium on Turbulent Shear Flows held in 1995.

References

Abe, K., Kondoh, T., Nagano, Y., 1997. On Reynolds-stress expressions and near-wall scaling parameters for predicting wall and homogeneous turbulent shear flows. Int. J. Heat Fluid Flow 18, 266–282.

Betts, P.L., Dafa'Alla, A.A., 1986. Turbulent buoyant air flow in a tall rectangular cavity. In: J.A.C. Humphrey et al. (Eds.), Significant Questions in Buoyancy Affected Enclosure or Cavity Flows, Anaheim, vol. 60, ASME HTD, New York, pp. 83–91.

Brereton, G.J., Mankbadi, R.R., 1993. A rapid-distortion-theory turbulence model for developed unsteady wall-bounded flow. In: R.M.C. So et al. (Eds.), Near-Wall Turbulent Flows, Elsevier, Amsterdam, pp. 95–104.

Brereton, G.J., Mankbadi, R.R., 1995. Development of a rapid-distortion turbulence model for unsteady hydrodynamic and scalar boundary layers. In: F. Durst et al. (Eds.), Proceedings of Tenth Symposium on Turbulent Shear Flows, Pennsylvania State University, pp. 21.7–21.12.

Cotton, M.A., Ismael, J.O., 1993. Development of a two-equation turbulence model with reference to a strain parameter. In: P.-L. Viollet et al. (Eds.), Proceedings of Fifth International Symposium on Refined Flow Modelling and Turbulence Measurements, Paris, pp. 117–124.

Cotton, M.A., Ismael, J.O., 1996. Initial formulation of a strain parameter closure for turbulent shear flows. University of Manchester Report (minor corrections January 1997).

Cotton, M.A., Jackson, J.D., 1990. Vertical tube air flows in the turbulent mixed convection regime calculated using a low-Reynolds-number k–ϵ model. Int. J. Heat Mass Transfer 33, 275–286.

Cotton, M.A., Kirwin, P.J., 1993. A comparative study of two-equation turbulence models applied to turbulent mixed convection in vertical pipes. In: P.-L. Viollet et al. (Eds.), Proceedings of Fifth International Symposium on Refined Flow Modelling and Turbulence Measurements, Paris, pp. 375–382.

Cotton, M.A., Kirwin, P.J., 1995. A variant of the low-Reynolds-number two-equation turbulence model applied to variable property mixed convection flows. Int. J. Heat Fluid Flow 16, 486–492.

Craft, T.J., Launder, B.E., Suga, K., 1996. Development and application of a cubic eddy-viscosity model of turbulence. Int. J. Heat Fluid Flow 17, 108–115.

Dean, R.B., 1978. Reynolds number dependence of skin friction and other bulk flow variables in two-dimensional rectangular duct flow. ASME J. Fluids Eng. 100, 215–223.

Finnicum, D.S., Hanratty, T.J., 1988. Influence of imposed flow oscillations on turbulence. PhysicoChemical Hydrodyn. 10, 585–598.

Gibson, M.M., Launder, B.E., 1978. Ground effects on pressure fluctuations in the atmospheric boundary layer. J. Fluid Mech. 86, 491–511.

Hall, W.B., Jackson, J.D., 1969. Laminarization of turbulent pipe flow by buoyancy forces. ASME Paper 69-HT-55.

Hunt, J.C.R., 1978. A review of the theory of rapidly distorted turbulent flows and its applications. Fluid Dynamics Trans. 9, 121–152.

Hunt, J.C.R., Carruthers, D.J., 1990. Rapid distortion theory and the 'problems' of turbulence. J. Fluid Mech. 212, 497–532.

Hunt, J.C.R., Maxey, M.R., 1978. Estimating velocities and shear stresses in turbulent flows of liquid metals driven by low frequency electromagnetic fields. In: H. Branover (Ed.), MHD Flows and Turbulence II, Israel Universities Press, Israel, pp. 249–269.

Jackson, J.D., Cotton, M.A., Axcell, B.P., 1989. Studies of mixed convection in vertical tubes. Int. J. Heat Fluid Flow 10, 2–15.

Jackson, J.D., He, S., 1995. Simulations of transient turbulent flow using various two-equation low-Reynolds-number turbulence models. In: F. Durst et al. (Eds.), Proceedings of Tenth Symposium on Turbulent Shear Flows, Pennsylvania State University, pp. 11.19–11.24.

Jones, W.P., Launder, B.E., 1972. The prediction of laminarization with a two-equation model of turbulence. Int. J. Heat Mass Transfer 15, 301–314.

Kim, J., 1990. See Rodi, W., Mansour, N.N., 1990. In: Studying Turbulence using Numerical Simulation Databases-III, Proceedings of 1990 Summer Program, Center for Turbulence Research, Stanford University, pp. 85–106; Michelassi, V., Rodi, W., Scheuerer, G., 1991. In: F. Durst et al. (Eds.), Presented at Eighth Symposium on Turbulent Shear Flows, Munich.

Kim, J., Moin, P., Moser, R., 1987. Turbulence statistics in fully developed channel flow at low Reynolds number. J. Fluid Mech. 177, 133–166.

Kirwin, P.J., 1995. Investigation and Development of Two-Equation Turbulence Closures with Reference to Mixed Convection in Vertical Pipes. Ph.D. Thesis, University of Manchester.

Launder, B.E., 1986. Low-Reynolds-number turbulence near walls. UMIST Report TFD/86/4.

Launder, B.E., Sharma, B.I., 1974. Application of the energy-dissipation model of turbulence to the calculation of flow near a spinning disc. Lett. Heat Mass Transfer 1, 131–138.

Launder, B.E., Spalding, D.B., 1972. Lectures in Mathematical Models of Turbulence. Academic Press, New York.

Launder, B.E., Spalding, D.B., 1974. The numerical computation of turbulent flows. Comp. Meth. Appl. Mech. Eng. 3, 269–289.

Lee, M.J., Kim, J., Moin, P., 1987. Turbulence structure at high shear rate. In: F. Durst et al. (Eds.), Proceedings of Sixth Symposium on Turbulent Shear Flows, Toulouse, Paper 22-6.

Lee, M.J., Kim, J., Moin, P., 1990. Structure of turbulence at high shear rate. J. Fluid Mech. 216, 561–583.

Leschziner, M.A., 1982. An introduction and guide to the computer code PASSABLE. UMIST Report.

Lumley, J.L., Berkooz, G., Elezgaray, J., Holmes, P., Poje, A., Volte, C., 1996. Fundamental aspects of incompressible and compressible turbulent flows. In: T.B. Gatski et al. (Eds.), Simulation and Modeling of Turbulent Flows, Oxford, pp. 5–78.

Mankbadi, R.R., Liu, J.T.C., 1992. Near-wall response in turbulent shear flows subjected to imposed unsteadiness. J. Fluid Mech. 238, 55–71.

Mansour, N.N., Kim, J., Moin, P., 1988. Reynolds-stress and dissipation-rate budgets in a turbulent channel flow. J. Fluid Mech. 194, 15–44.

Maxey, M.R., 1978. Aspects of Unsteady Turbulent Shear Flow, Turbulent Diffusion and Tidal Dispersion. Ph.D. Dissertation, University of Cambridge.

Maxey, M.R., 1982. Distortion of turbulence in flows with parallel streamlines. J. Fluid Mech. 124, 261–282.

Michelassi, V., Rodi, W., Scheuerer, G., 1991. Testing a low Reynolds number k–ϵ turbulence model based on direct simulation data. In:

F. Durst et al. (Eds.), Proceedings of the Eighth Symposium on Turbulent Shear Flows, Munich.

Patel, V.C., Head, M.R., 1969. Some observations on skin friction and velocity profiles in fully developed pipe and channel flows. J. Fluid Mech. 38, 181–201.

Patel, V.C., Rodi, W., Scheuerer, G., 1985. Turbulence models for near-wall and low Reynolds number flows: A review. AIAA J. 23, 1308–1319.

Petukhov, B.S., Polyakov, A.F., 1988. In: B.E. Launder (Ed.), Heat Transfer in Turbulent Mixed Convection. Hemisphere, Washington, DC.

Poškas, P.S., 1991. Personal communication.

Rodi, W., Mansour, N.N., 1990. Low Reynolds number k–ϵ modeling with the aid of direct simulation data. In: Studying Turbulence using Numerical Simulation Databases-III, Proceedings of 1990 Summer Program, Center for Turbulence Research, Stanford University, pp. 85–106.

Savill, A.M., 1987. Recent developments in rapid-distortion theory. Ann. Rev. Fluid Mech. 19, 531–575.

Savill, A.M., 1993. Some recent progress in the turbulence modelling of by-pass transition. In: R.M.C. So et al. (Eds.), Near-Wall Turbulent Flows. Elsevier, Amsterdam, pp. 829–848.

Spalart, P.R., Allmaras, S.R., 1994. A one-equation turbulence model for aerodynamic flows. Rech. Aérospat. 1, 5–21.

Speziale, C.G., 1987. On nonlinear k–l and k–ϵ models of turbulence. J. Fluid Mech. 178, 459–475.

Speziale, C.G., Mac Giolla Mhuiris, N., 1989. On the prediction of equilibrium states in homogenous turbulence. J. Fluid Mech. 209, 591–615.

Tavoularis, S., Corrsin, S., 1981. Experiments in nearly homogeneous turbulent shear flow with a uniform mean temperature gradient. Part 1. J. Fluid Mech. 104, 311–347.

Townsend, A.A., 1970. Entrainment and the structure of turbulent flow. J. Fluid Mech. 41, 13–46.

Vilemas, J.V., Poškas, P.S., Kaupas, V.E., 1992. Local heat transfer in a vertical gas-cooled tube with turbulent mixed convection and different heat fluxes. Int. J. Heat Mass Transfer 35, 2421–2428.